Available online at www.sciencedirect.com
ScienceDirect
Carbohydrate Research 342 (2007) 2593–2598
Carbohydrate RESEARCH

Molecular imaging of single cellulose chains aligned on a highly oriented pyrolytic graphite surface

Shingo Yokota, Tomotsugu Ueno, Takuya Kitaoka* and Hiroyuki Wariishi

Department of Forest and Forest Products Sciences, Graduate School of Bioresource and Bioenvironmental Sciences, Kyushu University, Fukuoka 812-8581, Japan

Received 9 July 2007; received in revised form 18 August 2007; accepted 20 August 2007
Available online 31 August 2007

Abstract—Individual cellulose macromolecules were successfully visualized on a highly oriented pyrolytic graphite (HOPG) surface by tapping-mode atomic force microscopy under ambient condition. Monomolecular-level dispersion of cellulose chains was achieved through the momentary contact of dilute cellulose/cupri-ethylenediamine (Cu-ED) solution onto the HOPG substrate. Both concentrations of cellulose and Cu-ED provided critical impacts on the topographical images. Single cellulose chains with molecular height of ca. 0.55 nm could be observed under the optimal conditions, showing rigid molecular rods with a unique morphology of hexagonal regularity. It was strongly suggested that the cellulose chains were aligned along the HOPG crystal lattice through a specific attraction, possibly due to a CH–π interaction between the axial plane of cellulose and the HOPG π-conjugated system. These phenomena would imply the potential applications of an HOPG substrate for not only nano-level imaging, but also for molecular alignment of cellulose and other structural polysaccharides.

Keywords: Cellulose; Nano-imaging; Molecular alignment; Highly oriented pyrolytic graphite; Atomic force microscopy

1. Introduction

The morphological nano-imaging of biomacromolecules at the single molecular level provides various kinds of fundamental information on biological and physicochemical aspects, resulting in a number of innovative possibilities for the development of functional biopolymer materials.[1,2] Atomic force microscopy (AFM), one of the major scanning probe microscopic analyses, is a powerful tool for molecular imaging under various analytical conditions. AFM visualization offers the conformational details of individual polymers on the nano-flat substrates at an atomic resolution, especially in the vertical direction.[3] Hence, nano-imaging via AFM has recently attracted much attention for determining the sharp distinction of real shapes of macromolecules and their assembly, being complementary to the conventional analytical methods providing the average information on polymer population, for example, light scattering, viscoelastic, spectroscopic and chromatographic characteristics.[4]

Many researchers have currently reported that moderate interaction at the polymer/substrate interface is an essential factor for successful AFM imaging without any displacement and distortion of the polymer samples.[3] Cleaved mica and highly oriented pyrolytic graphite (HOPG) are typical atomically-smooth substrates for the AFM imaging of hydrophilic and hydrophobic polymers, respectively. In the case of deoxyribonucleic acid (DNA) imaging, anionic DNA chains were successfully attached onto the negatively-charged mica surface through an electrostatic screening via cationic mediators.[5–7] On the other hand, it was reported that hydrophobic *n*-alkane-grafted polymers were regularly oriented on an HOPG surface via hydrophobic interaction, and their epitaxial crystallization was visualized by AFM analysis.[8–10] Thus, AFM imaging can provide a significant insight into the fundamental knowledge of polymer characteristics.

* Corresponding author. Tel./fax: +81 92 642 2993; e-mail: tkitaoka@agr.kyushu-u.ac.jp

0008-6215/$ - see front matter © 2007 Elsevier Ltd. All rights reserved.
doi:10.1016/j.carres.2007.08.018

Cellulose is the most abundant biomacromolecule, and forms the main constituent of the cell wall in higher plants.[11] Cellulosic polymers have been widely used in a diverse array of applications, for example, in paper, textile fibres, film, plastics, food additives, cosmetics and medical supplies.[12] Recently, the molecular features of cellulose for self-assembly and hierarchical organization have generated much interest in the area of smart materials from bio- and nano-engineering perspectives.[12,13] The three equatorially-positioned hydroxyl groups of the anhydroglucopyranose (AHG) unit in the cellulose β-(1 → 4)-D-glucan-chains trigger the spontaneous formation of a regular and strong hydrogen-bonding network, resulting in the vertical stacking of hydrophobic axial faces mainly through van der Waals attraction.[14–16] Such molecular assembling features lead to poor solvent solubility, and thus the strong molecular interaction makes the AFM observation of individual cellulose chains much more difficult. Successful molecular imaging of various water-soluble polysaccharides has been more or less achieved,[17–20] but not yet for cellulose.

Recently, we reported very clear AFM images of carboxymethylcellulose (CMC), a typical water-soluble (hydrophilic) cellulose ether derivative, by using a hydrophobic HOPG substrate.[21] The conformational changes in individual CMC chains were successfully visualized under various salt conditions, where the residual AHG units in the CMC chains possibly played an important role in the moderate CMC attachment onto the HOPG surface for clear molecular imaging. In this study, we challenged the molecular imaging of single cellulose chains by tapping-mode AFM analysis using a hydrophobic HOPG substrate. Homogeneous cellulose/cupri-ethylenediamine (Cu-ED) solution was placed in momentary contact with the HOPG surface, enabling the physical adsorption of molecular cellulose on the HOPG surface. The morphological changes in cellulose chains at a mono-molecular level were investigated by altering the Cu-ED and cellulose concentrations.

2. Results and discussion

2.1. Effect of Cu-ED concentration on cellulose visualization

In general, water-soluble polymer chains can be simply placed on a hydrophilic mica surface by applying the polymer solution dropwise, and in most cases AFM observation is possible by controlling the solution conditions.[3] However, this conventional approach was not effective for AFM imaging of CMC[21] and cellulose (data not shown), possibly due to their strong molecular assembling properties, although cellulose is homogeneously soluble in aqueous 500 mM Cu-ED solution in a complex state, as illustrated in Figure 1.[22] Hence, the hydrophobic HOPG substrates were applied to adequately immobilize the cellulose chains for AFM imaging.

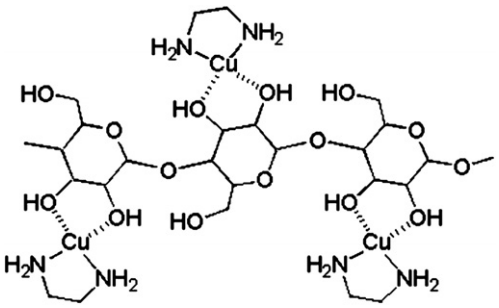

Figure 1. Schematic illustration of cellulose coordinated with the cupri-ethylenediamine complex (Cu-ED) at its C-2 and C-3 hydroxyl groups.[22]

Figure 2a shows the AFM image of the HOPG surface treated with 20 mg L^{-1} cellulose/500 mM Cu-ED solution. Long-chain cellulose with a molecular weight (MW) of ca. 2.8×10^5 g mol^{-1} was subjected to the AFM imaging. Disordered tangled cellulose chains were observed, but molecular imaging was possible to some extent under the conditions that no cellulose chains were found on the mica substrate. Nothing was also found on the HOPG substrate treated with cellulose-free 500 mM Cu-ED solution, and X-ray photoelectron spectroscopy (XPS) of the HOPG surface of Figure 2a confirmed that there was no elemental peak of Cu and N derived from Cu-ED solution (see Supplementary data). Thus, residual Cu-ED portions were little as to be neglected within the limit of XPS detection, probably indicating that most of the cellulose/Cu-ED coordination was cleaved by sufficiently rinsing with water. As in the case of the previous CMC study,[21] a successful AFM imaging could be achieved by adjusting the contact time of the cellulose droplet on the HOPG surface (within 1 s); a shorter contact time achieves better molecular dispersion. In all cases for the AFM imaging, longer contact times brought about excessive adsorption and massive aggregation of cellulose molecules and their assembly, resulting in an obscure molecular imaging because of the overall coverage of the HOPG surface (data not shown).

Lowering the Cu-ED concentration at the same cellulose content (20 mg L^{-1}) provided the different AFM images shown in Figure 2b–e. In the case of 250 mM Cu-ED concentration, a wire net-like assembly with flexible cellulose chains was observed (Fig. 2b), while the regular nano-network morphology comprised of linearly-ordered polymer segments was found in the AFM image of the HOPG surface treated with the 100 mM Cu-ED solution (Fig. 2c and d). Molecular-level cellulose chains of 0.58–1.28 nm thickness were confirmed by the vertical information of the AFM image, that is, a height profile along the white line indicated in Figure

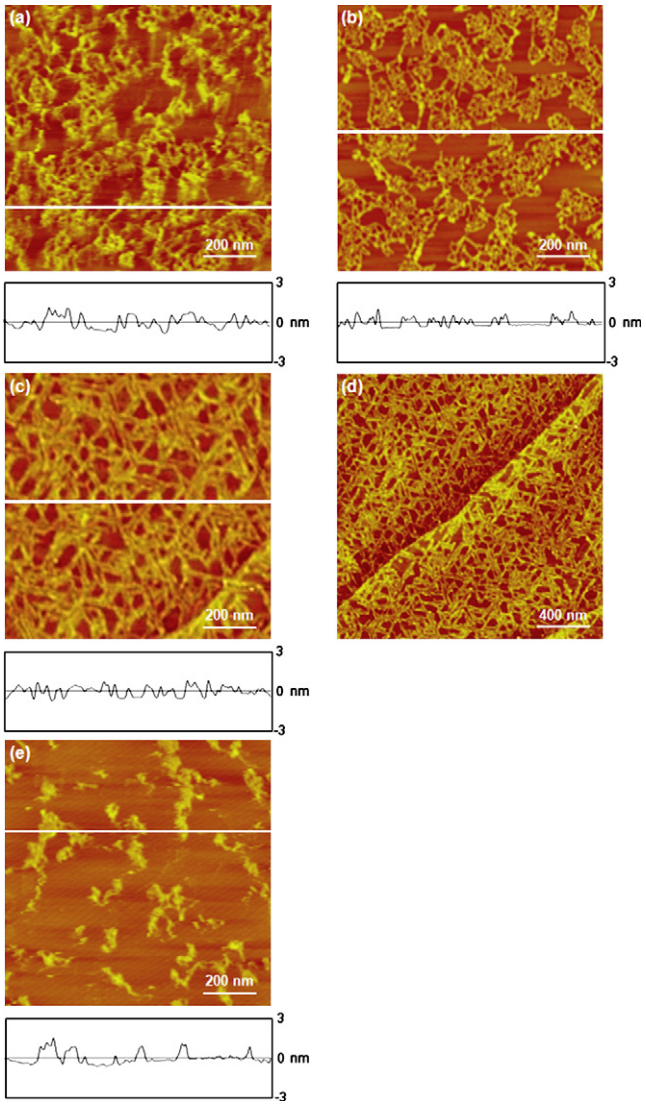

Figure 2. AFM images of cellulose chains on the HOPG substrate treated with 20 mg L^{-1} long-chain cellulose/Cu-ED solution. Cu-ED concentration: (a) 500 mM, (b) 250 mM, (c, d) 100 mM and (e) 80 mM. Image size: (a–c, e) 1.0×1.0 μm^2 and (d) 2.0×2.0 μm^2. Height profiles along the scanning (white) lines are indicated below each AFM image.

2c. Further dilution of the Cu-ED solution (80 mM) brought about the larger, non-fibrous aggregation of cellulose chains possibly due to the insufficient dissolution (Fig. 2e).

In the cellulose/Cu-ED/H_2O system, it is well known that the molecular dispersion of cellulose is achieved by the disruption of intra- and inter-molecular hydrogen bonds via the stoichiometric coordination of the Cu-ED complex to C-2 and C-3 hydroxyl groups of cellulose, as illustrated schematically in Figure 1.[22] Thus, cellulose chains dissolved in the Cu-ED solution with higher concentration were possibly deprived of their molecular rigidity (Fig. 2a). On the other hand, cellulose molecules were presumably obtained in their original amphiphilic ribbon-shaped conformation at a lower Cu-ED concentration by diluting the solution. Cellulose chain alignment on the HOPG surface in 100 mM Cu-ED (Fig. 2c and d) was similar to that of CMC mono-chains reported in our previous study,[21] indicating that rigid cellulose polymers strongly interacted with the HOPG surface through a specific attraction. Obvious deposition of cellulose was found at an 80 mM Cu-ED concentration (Fig. 2e) due to the excess dilution possibly inducing the formation of an unstable cellulose/Cu-ED complex. Thus, in this study, using long-chain cellulose with a MW of ca. 2.8×10^5 g mol^{-1}, a 100 mM Cu-ED solution obtained by fivefold diluting a 500 mM Cu-ED solution was the optimal solution for achieving appropriate molecular attachment and clear AFM imaging.

2.2. Molecular imaging of single cellulose chains

Morphological changes in single cellulose chains dispersed on the HOPG surface from 100 mM Cu-ED solution were investigated in detail as a function of cellulose concentration. Changes in the cellulose concentration ranging from 2.5 to 40 mg L^{-1} significantly affected the apparent molecular images of cellulose chains attached on the HOPG surfaces (Figs. 2c, d and 3). Needle-like cellulose chains were observed at 2.5 mg L^{-1} (Fig. 3a and b), and a nano-network morphology with rigid chain conformation was prominently displayed at 5.0 mg L^{-1} (Fig. 3c and d), being comparable to the case of 20 mg L^{-1} (Fig. 2c and d). Such nano-web morphology with a regular chain alignment was also found at a higher cellulose concentration (40 mg L^{-1}) but significantly became denser, as shown in Figure 3e and f. These results possibly indicated that the cellulose/HOPG interaction was considerably strong, driving the regular chain alignment in spite of the inherent cellulose/cellulose association. As indicated in Figures 2c, d and 3, the cellulose concentration was one of the critical factors for the molecular imaging of individual cellulose chains in the AFM analysis, and lower cellulose concentration brought about the good molecular dispersion of cellulose at a mono-chain level.

AFM imaging emphasizes the vertical profiles of polymer chains at an atomic resolution,[3] while conventional transmission electron microscopy offers poor contrast for carbohydrate polymers on a graphite surface. In order to distinguish individual cellulose chains, the molecular thickness of cellulose chains on the HOPG surface was measured in detail at 2.5 mg L^{-1}. In Figure 3a and b, well-scattered fine cellulose chains had a height of 0.55 ± 0.09 nm ($n = 40$), approximately corresponding to the thickness in the axial direction of cellobiose unit as predicted in theory by standard space filling model (0.4–0.5 nm).[23] It was also reported that

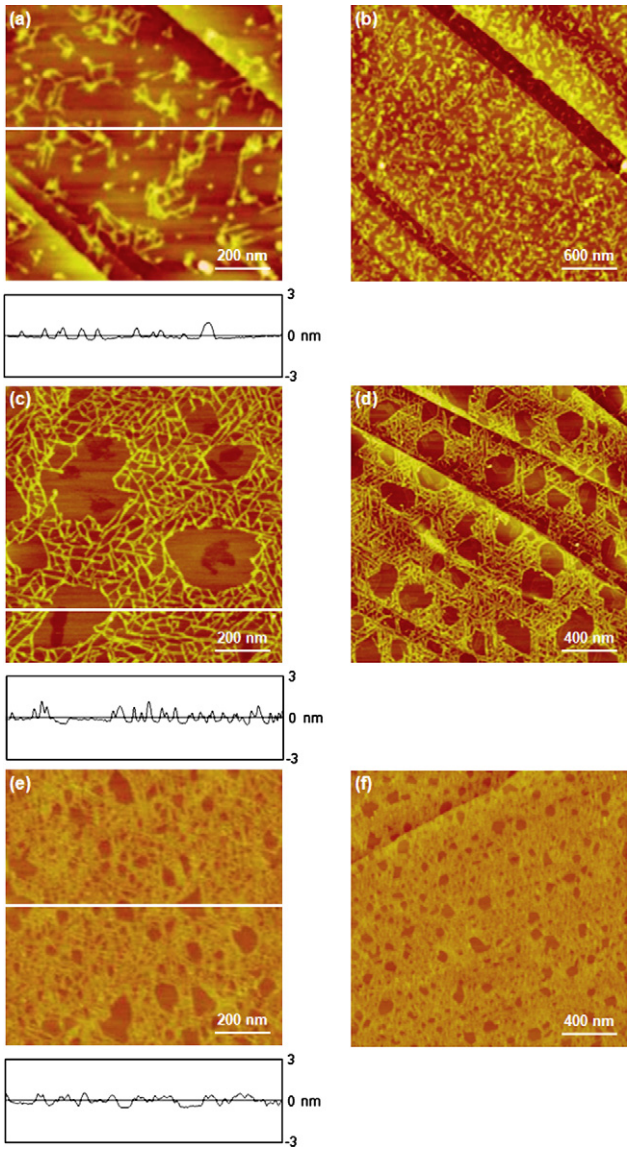

Figure 3. AFM images of cellulose chains on the HOPG substrate treated with long-chain cellulose/100 mM Cu-ED solution. Cellulose concentration: (a, b) 2.5 mg L^{-1}, (c, d) 5.0 mg L^{-1} and (e, f) 40 mg L^{-1}. Image size: (a, c, e) 1.0×1.0 μm^2, (b) 3.0×3.0 μm^2 and (d, f) 2.0×2.0 μm^2. Height profiles along the scanning (white) lines are indicated below each AFM image.

the *d*-spacing of (200) lattice plane of cellulose I_β was ca. 0.4 nm,[24] supporting the successful visualization of the single cellulose molecules attached on the HOPG surface. The rigid chain segments of the bendable molecular cellulose rods had a length of 60 ± 15 nm ($n = 40$), roughly comparable to the Kuhn length (ca. 20–30 nm) of cellulose dissolved in Cu-amine solution.[25] In the case of short-chain cellulose with a MW of ca. 3.2×10^4 g mol^{-1}, linear oriented cellulose bundles assembled with two or more molecules were illustrated in Figure 4, and most of the linear cellulose bundles, except for obscure dots and entanglements, possessed a

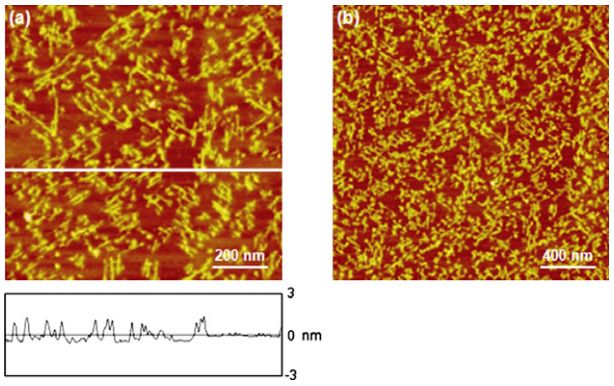

Figure 4. AFM images of cellulose chains on the HOPG substrate treated with 2.5 mg L^{-1} short-chain cellulose/50 mM Cu-ED solution. Image size: (a) 1.0×1.0 μm^2 and (b) 2.0×2.0 μm^2. Height profile along the scanning (white) line is indicated below AFM image (a).

longitudinal length of ca. 120 nm in rough accordance with the theoretical chain length (100–150 nm) of a native cellulose microfibril with level-off MW.[12] Thus, it was presumed that the AFM imaging in this study possibly provided the molecular shape of cellulose chains.

2.3. Molecular alignment of cellulose chains on HOPG

The molecular attachment of cellulose chains onto the HOPG surface appeared regularly, and similar molecular alignment was observed in Figures 2c, d, and 3c, d. Thus, the two-dimensional fast Fourier transformation (2D-FFT) analysis of the same HOPG facet (white square region), as shown in Figure 5a (the same AFM image in Fig. 2c), was performed to elucidate the directional characteristics for the cellulose/HOPG interaction. As shown in Figure 5b, the 2D-FFT diagram of the AFM image displayed a clear hexagonal pattern with three vectorial components crossing at 120° to each

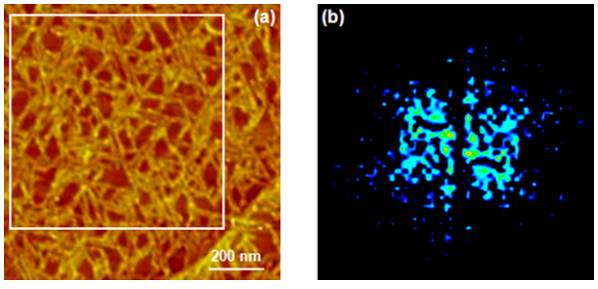

Figure 5. AFM and two-dimensional fast Fourier transform (2D-FFT) images of cellulose chains on the HOPG substrate treated with 20 mg L^{-1} long-chain cellulose/100 mM Cu-ED solution. (a) The same image as Figure 2c. (b) 2D-FFT was performed for the white square region in AFM image (a) to avoid any artifact calculation due to a gap in the different HOPG facets.

other. This result presumably suggested that the cellulose chains were aligned along the hexagonal HOPG crystal geometry with the sp^2 hybridized orbital of the aromatic rings. In Figure 3c and d, there were bare HOPG surface domains on which no cellulose chains were adsorbed, possibly implying that the quasi-rigid cellulose molecules were immediately stripped from the structural defect domains of the HOPG surface during the sample preparation.

An epitaxial array of *n*-alkane crystals on the HOPG surface has already been reported; the length of the C–C–C bonds of the *n*-alkane (0.251 nm) adapted to the unit cell size along the [10-10] axis of the HOPG crystal (0.246 nm) caused the *n*-alkane side-chains of the polymer to stand in a specific direction as a result of CH–π interaction.[8,9] It is also reported that the axial planes of ribbon-shaped cellulose strongly interact with the sp^2 hybridized orbital of the aromatic rings possibly due to CH–π bonding.[26,27] Hence, quasi-planar cellulose chains with a molecular rigidity owing to intra-molecular hydrogen bonds may match the planar graphite rings. The *c*-axis length of the native cellulose I_β crystal unit lattice (1.036 nm)[15,24] roughly corresponds to the fourfold length of the HOPG lattice parameter (0.984 nm). There may be a possibility that cellulose chains dissolved in 100 mM Cu-ED solution remained in their rigid but slightly flexible molecular structure, and were aligned on the HOPG crystal surface composed of a π-conjugated system via agreement with the geometric regularity of cellulose and HOPG during the molecular attachment of cellulose chains on the HOPG surface by cleaving the Cu-ED coordination. Such hexagonal molecular conformation was a unique specific morphology, and other β-(1 → 4)-D-glucan-type structural polysaccharides are expected to apply to the molecular imaging and alignment through the use of a hydrophobic HOPG substrate.

3. Conclusion

Single molecular cellulose chains were successfully immobilized on the HOPG surface and clearly visualized through AFM analysis, by carefully adjusting the contact time of the cellulose/Cu-ED solution with the HOPG surface. The molecular conformation and alignment of cellulose chains significantly varied with Cu-ED and cellulose concentrations. The angular hexagonal morphology of cellulose was observed; quasi-rigid cellulose chains were presumably attached onto the HOPG surface via CH–π interactions. The first achievement of the clear visualization of individual cellulose molecules by using a hydrophobic HOPG substrate would provide fundamental and valuable information on both the nano-imaging and molecular orientation of various structural polysaccharides.

4. Experimental

4.1. Materials

Commercial cotton cellulose samples (MW: ca. 2.8×10^5 and ca. 3.2×10^4 g mol^{-1}) were used after washing thoroughly with acetone; these were called long-chain and short-chain cellulose, respectively. Nano-flat HOPG plates were purchased from Veeco Instruments, Co. Ltd. The water used in this study was purified with a Milli-Q system (Millipore, Co. Ltd). Other chemicals were of extra-pure reagent grade and used without further purification.

4.2. Sample preparation

Cotton cellulose was dissolved in 1 M Cu-ED aqueous solution at room temperature for more than 24 h, followed by diluting twice with Milli-Q water according to the conventional method.[28] The working solution was prepared with 80–500 mM Cu-ED solution (final concentration of cellulose: 2.5–40 mg L^{-1}) from 2 g L^{-1} cellulose/500 mM Cu-ED solution stored at 4 °C for more than 48 h. A small amount of designated cellulose/Cu-ED solution (10 μL) was dropped onto acetone-prewashed HOPG at room temperature, and immediately removed within 1 s by waving in air, followed by sufficiently rinsing with Milli-Q water and drying in a stream of dry N_2 gas.

4.3. AFM Imaging

AFM topographical images were obtained under ambient conditions using a NanoScope IIIa atomic force microscope (Digital Instruments, Co. Ltd) operated by tapping mode with an E-type scanner and single-crystal silicon cantilevers (length: 125 μm, spring constant: 40 N m^{-1}, resonance frequency: 200–400 kHz). AFM measurements were carried out at five different regions (scan size: 1.0×1.0, 2.0×2.0, 3.0×3.0 μm^2) per sample. The morphological data of the AFM images, that is, height and length were analyzed using the AFM-accessory software (ver. 5.12b36), and two-dimensional fast Fourier transformation (2D-FFT) was performed via a Scanning Probe Image Processor (SPIP ver. 3.1.0.2, Image Metrology A/S). All AFM images presented here were adequately flattened using the software to correct the distortion at a micrometer scale, but no other digital operation was carried out.

Acknowledgements

This research was supported by a Research Fellowship of the Japan Society for the Promotion of Science for Young Scientists (S.Y.) and by a Grant-in-Aid for

Young Scientists (No. 17688008) from the Ministry of Education, Culture, Sports, Science and Technology (MEXT), Japan (T.K.).

Supplementary data

Supplementary data associated with this article can be found, in the online version, at doi:10.1016/j.carres.2007.08.018.

References

1. Ellis, J. S.; Allen, S.; Chim, Y. T. A.; Roberts, C. J.; Tendler, S. J. B.; Davies, M. C. *Adv. Polym. Sci.* **2006**, *193*, 123–172.
2. Abu-Lail, N. I.; Camesano, T. A. *J. Microsc.* **2003**, *212*, 217–238.
3. Binning, G.; Quate, C. F.; Gerber, C. *Phys. Rev. Lett.* **1986**, *6*, 930–933.
4. Wilkinson, K. J.; Balnois, E.; Leppard, G. G.; Buffle, J. *Colloids Surf., A* **1999**, *155*, 287–310.
5. Helen, G. H.; Daniel, E. L. *Biophys. J.* **1996**, *70*, 1933–1939.
6. Shlyakhtenko, L. S.; Gall, A. A.; Weimer, J. J.; Hawn, D. D.; Lyubchenko, Y. L. *Biophys. J.* **1999**, *77*, 568–576.
7. Podesta, A.; Imperadori, L.; Colnaghi, W.; Finzi, L.; Milani, P.; Dunlap, D. *J. Microsc.* **2004**, *215*, 236–240.
8. Hooks, D. E.; Fritz, T.; Ward, M. D. *Adv. Mater.* **2001**, *13*, 227–241.
9. Imase, T.; Ohira, A.; Okoshi, K.; Sano, N.; Kawauchi, S.; Watanabe, J.; Kunitake, M. *Macromolecules* **2003**, *36*, 1865–1869.
10. Percec, V.; Rudick, J. G.; Wagner, M.; Obata, M.; Mitchell, C. M.; Cho, W.; Magonov, S. N. *Macromolecules* **2006**, *39*, 7342–7351.
11. Kadla, J. F.; Gilbert, R. D. *Cellul. Chem. Technol.* **2000**, *34*, 197–216.
12. Klemm, D.; Heublein, B.; Fink, H.-P.; Bohn, A. *Angew. Chem., Int. Ed.* **2005**, *44*, 3358–3393.
13. Klemm, D.; Schumann, D.; Kramer, F.; Heßler, N.; Hornung, M.; Schmauder, H.-P.; Marsch, S. *Adv. Polym. Sci.* **2006**, *205*, 49–96.
14. Jarvis, M. *Nature* **2003**, *426*, 611–612.
15. Nishiyama, Y.; Langan, P.; Chanzy, H. *J. Am. Chem. Soc.* **2002**, *124*, 9074–9082.
16. Nishiyama, Y.; Sugiyama, J.; Chanzy, H.; Langan, P. *J. Am. Chem. Soc.* **2003**, *125*, 14300–14306.
17. Decho, A. W. *Carbohydr. Res.* **1999**, *315*, 330–333.
18. Balnois, E.; Stoll, S.; Wilkinson, K. J.; Buffle, J.; Rinaudo, M.; Milas, M. *Macromolecules* **2000**, *33*, 7440–7447.
19. Camesano, T. A.; Wilkinson, K. J. *Biomacromolecules* **2001**, *2*, 1184–1191.
20. Spagnoli, C.; Korniakov, A.; Ulman, A.; Balazs, E. A.; Lyubchenko, Y. L.; Cowman, M. K. *Carbohydr. Res.* **2005**, *340*, 929–941.
21. Ueno, T.; Yokota, S.; Kitaoka, T.; Wariishi, H. *Carbohydr. Res.* **2007**, *342*, 954–960.
22. Miyamoto, I.; Inamoto, M.; Matsui, T.; Saito, M.; Okajima, K. *Polym. J.* **1995**, *27*, 1113–1122.
23. Kondo, T.; Togawa, E.; Brown, R. M. *Biomacromolecules* **2001**, *2*, 1324–1330.
24. Sugiyama, J.; Vuong, R.; Chanzy, H. *Macromolecules* **1991**, *24*, 4168–4175.
25. Burchard, W.; Habermann, N.; Klüfers, P.; Seger, B.; Wilhelm, U. *Angew. Chem., Int. Ed. Engl.* **1994**, *33*, 884–887.
26. Glennon, T. M.; Mertz, K. M. *J. Mol. Struct. (THEOCHEM)* **1997**, *395*, 157–171.
27. Palma, R.; Himmel, M. E.; Brady, J. W. *J. Phys. Chem. B* **2000**, *104*, 7228–7234.
28. *Tech. Assoc. Pulp Pap. Ind. Test Methods* **1997**, T230.